Surface Phonon Polariton Modes in Suspended Monolayer Hexagonal Boron Nitrides

M. Y. Musa[1], G. S. Shehu[2*], M. A. Husein[3], M. Imran[4], H. B. Murtala[5], Y. Jibril[2]

[1]Department of Mechanization and Engineering, Audu Bako College of Agriculture, Kano, Nigeria.
[2]Department of Electrical Engineering, Ahmadu Bello University Zaria, Nigeria.
[3]Department of Electrical and Computer Engineering, Baze University Abuja, Nigeria
[4]Department of Electronics, University of Buner Khyber Pukhunkhwam, Pakistan.
[5]Department of Electrical Engineering, Federal University Gusau, Nigeria

ABSTRACT: Dispersion properties and characteristics of transverse magnetic (TM) and transverse electric (TE) surface phonon polaritons (SPhP) in suspended monolayer hexagonal boron nitrides (hBN) was studied extensively. The analytical results show that the hBN based TM (TE) phonon polaritons exist in restsrahlen bands when imaginary surface conductivity is positive. The effective mode index of TM phonon polaritons is much higher than that of TE phonon polaritons with respective values of ~ 3000 and ~ 1.0002 which makes TM SPhP more promising in the practical realization. In addition, the propagation length of TE SPhP is less lossy and surpass that of TM SPhP by factor of 10^4. This study compares these important properties and sheds more insight into their applications in optical communications, photonics and optoelectronics devices.

KEYWORDS: Phonon polaritons, hexagonal boron nitrides, skin depth, transverse electric, ultrathin

[Received Aug. 8, 2020; Revised March 2, 2021; Accepted May 12, 2021] Print ISSN: 0189-9546 | Online ISSN: 2437-2110

I. INTRODUCTION

Phonon polaritons are quasi-particles that resulted from strong hybridization of light-photons with collective lattice vibration in polar crystals. The physical feature of the surface polaritons phenomena are extreme field enhancement which results into subwavelength squeezing of light wavefront and nano device designs (Zhang et al., 2012; Duong Thi Ha et al., 2017; Caldwell et al., 2015). It also enables most of modern electronics and photonics phenomena such as lithography, electronics miniaturization, nanophotonics, and light manipulations (Hong, et al., 2019; Zhang et al., 2014). The representative polar crystal is hexagonal boron nitrides (hBN) – white graphite, which is wide band gap semiconductor with interested optical, mechanical and electronics properties (Cassabois et al., 2016; Kim et al., 2012). The major advantage of hBN as representative of two-dimensional polar crystal is due to the possibility of exfoliating it to monolayer, with thickness of 0.34 nm as require in the design process (Wickramaratne, et al., 2018). This capability of exfoliating hBN crystal to the monolayer led to the design of nanoelectronics and nanophotonics devices. Similar to fundamental waveguide modes in bulk semiconductors, phonon polaritons in two-dimensional (2d) hBN exhibit wave-like propagation in fundamental and subsequent high-order modes. This prompt usage of 2d hBN in applications such as sensors, nano-imaging, lithography, anomalous refraction, reflection, and emitters (Poddubny et al., 2013; Shi, 2014).

In polar crystals, Restsrahlen bands (RB) are narrow bands that are characterized with strong interaction of light with the materials. The longitudinal and transverse optical phonons abbreviated as LO and TO respectively are upper and lower boundaries of the RBs. The changing signs of real part of permittivity from positive to negative highlights strong optical phonon and photon coupling. This takes place in two different optical axes (parallel or perpendicular) to signify strong anisotropic property of the hBN. Within hBN crystal, the first and second RB bounded respectively between $21 > f > 24$ THz and $39 > f > 41$ THz. The sign of real permittivity for the out-of-plane is negative in the first RB ($\varepsilon_{\perp}$), it is also negative for the in-plane optical axis in the second RB ($\varepsilon_{\parallel}$).

The advent of nanophotonics in two-dimensional materials widen the continue research and integration of two-dimensional based polaritons. Numerous potential proof-of-concept designs and unusual phenomena are possible in monolayer, few layers, and heterostructures of these exotic materials (Basov et al, 2016; Dai et al., 2014). Plasmon polaritons in metals, semimetals, and semiconductors are the pioneers in the field from the first reported exfoliation of monolayer graphene (Low et al., 2017; Basov et al., 2016). Exciton polaritons in the cavity and surface of the transition metal-dicalchogenides (TMD) are also gaining attention especially in solar photovoltaic and optoelectronics (Mak et al., 2016). There is also magnon polaritons in magnetic

*Corresponding author: gsshehu@abu.edu.ng
doi: http://dx.doi.org/10.4314/njtd.v18i2.4

materials, and cooper pair polaritons in superconducting materials (Low, et al., 2017). Hybrid polaritons are extremely significant in numerous potentials such as plasmon-phonons between graphene and hBN, plasmon-excitons between graphene and TMD, then possibly phonon-excitons between hBN and TMDs (Low et al., 2017). In this work, we conceptually analyzed the two fundamental phonon polaritons modes in monolayer hBN, as described in the methods and conclusions.

II. METHODS

Unlike bulk polaritons, two-dimensional polaritons are mostly defined based on the sign of imaginary surface conductivity of the ultrathin materials. This facilitates easier characterization of two-dimensional polaritons in the atom-thick materials. Within electrodynamic analysis, Maxwell's equations are employed to define the 2d material as the surface conducting sheet σ_s using surface conductivity, the well-known real part of permittivity is unrealistic in 2d materials characterization. When the sign of imaginary surface conductivity is positive, the transverse magnetic phonon polaritons can be expected within the frequency band, while it is transverse electric phonon polaritons for the negative imaginary surface conductivity (Musa et al., 2017; Lin et al., 2017).

The analysis is started with deriving the dispersion relation of the TM phonon polaritons of suspended monolayer hBN as shown in Figure 1. The suspended structure means both superstrate and substrate are filled with vacuum ($\varepsilon_r = 1$) in each of the half-spaces. The alignment of the structure is considered to be perpendicular to the optical axis and represented analytically with σ_s as metallic conducting sheet. This is due to the fact that at RB, the hBN crystal reflects incident lights.

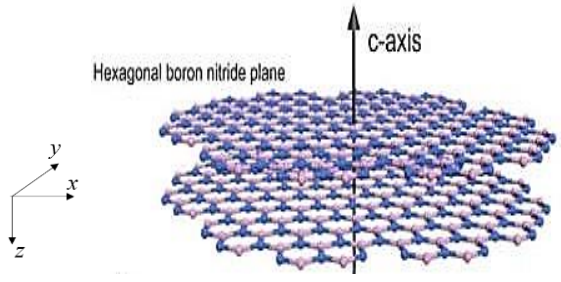

Figure 1: Suspended monolayer hexagonal boron nitrides, which can be represented with surface conductivity σ_s.

The electromagnetic wave incident onto the crystal propagates in *x*-direction and decays in *z*-direction. The analytical representation of the EM wave is written as $\bar{H}_{1y} = A_1 e^{-ik_{1z}z} e^{-k_x x}$ and $\bar{H}_{2y} = A_2 e^{ik_{2z}z} e^{-k_x x}$ for the upper and lower half-spaces respectively. The electric field components which corresponds to each half-spaces can be obtained using the relation $\bar{E} = \frac{-k \times \bar{H}_y}{\omega \varepsilon_0 \varepsilon_{1,2}}$, where $k = \hat{x}k_x + \hat{y}k_y + \hat{z}k_z$ and ε_0 is the permittivity of free space. After algebraic simplification, the TM SPhP modes characteristics equation of monolayer hBN is:

$$\frac{k_{1z}}{\varepsilon_1} + \frac{k_{2z}}{\varepsilon_2} - \frac{\sigma_s}{\omega \varepsilon_0} \frac{k_{1z}}{\varepsilon_1} \frac{k_{2z}}{\varepsilon_2} = 0 \quad (1)$$

where $k_{1,2z} = \sqrt{(\varepsilon_{1,2} k_0^2 - k_x^2)}$, $k_0 = \frac{\omega}{c}$, and $c = 3 \times 10^8\ m/s$. The wave vectors $k_{1,2z}$ and k_x are the transverse and longitudinal (propagating) wave vectors respectively. Equation 1 describes the relationship of frequency (ω) and the propagation wave vector (k_x). From the field equations $\bar{H}_{1,2y}$ it can be seen that the electric field components are parallel to the material plane while magnetic field is transverse. This has important physical application in the excitations and integration of these modes to the on-chip optoelectronics devices.

Similarly, to derive dispersion relation of the TE SPhP wave, the electric field components are transverse to the propagation direction. For the upper and lower half-spaces can be written as $\bar{E}_{1y} = A_1 e^{-ik_{1z}z} e^{-k_x x}$ and $\bar{E}_{2y} = A_2 e^{ik_{2z}z} e^{-k_x x}$ respectively. The corresponding magnetic field component can be obtained from $\bar{H} = \frac{k \times \bar{E}_y}{\omega \mu_0}$, with μ_0 is the vacuum permeability, and the system is considered to be nonmagnetic. Following analytic simplification, the dispersion relation of TE SPhP is obtained as;

$$k_{z1} + k_{z2} + \sigma_s \omega \mu_0 = 0 \quad (2)$$

From the TE dispersion relation in Equation 2, one can intuitively to depict the polarization of electric and magnetic fields components. The electric field component is transverse to the material plane in this case, while magnetic field components are parallel. For an ultrathin hBN crystal, there is absence of statistical model that define the surface conductivity like that of graphene. The relative permittivity model can be used to obtain the surface conductivity expression as follows (Lee et al, 2014a; Lee et al., 2014b):

$$\sigma_s = \left[\varepsilon_{r\perp,\mathrm{hBN}}(\omega) - \varepsilon_{r\perp}(\infty)\right] \varepsilon_0 \omega d \quad (3)$$

where $\varepsilon_{r\perp}(\infty) = \lim_{\omega \to \infty} \varepsilon_{r,\mathrm{hBN}}(\omega) = 4.87$ (Musa et al, 2017), and the thickness of hBN sheet is represented by *d*. The relative in-plane permittivity of hBN is given: $\varepsilon_{r\perp,hBN}(\omega) = \varepsilon_{r\perp}(\infty) + s_v \frac{{\omega^2}_v}{{\omega^2}_v - i\gamma_v \omega - \omega^2}$ as (Woessner et al., 2015). The constant parameters and their values in the expression are the vibrational frequency $\hbar\omega_v = 170.1$ meV, $\hbar$ is the reduced Planck's constant, the coupling factor $s_v = 1.83$, and finally the amplitude decay rate $\hbar\gamma_v = 0.87$ meV.

III. RESULTS AND DISCUSSION

The imaginary part of surface conductivity $Im(\sigma_s)$ depicts the type of transverse modes that can be sustained in the two-dimensional materials. When the $Im(\sigma_s)$ is positive, the corresponding real part of permittivity is negative and

describes strong light-matter coupling regime of the materials. Such regions are characterized with high reflection of light analogue to that of metal. This is akin to TM SPhP modes in metals or waveguides. However, when the $Im(\sigma_s)$ becomes negative, it is characterized with capacitive property. The rare but significant waveguide mode can be sustained with high and positive real part of permittivity. It is termed TE SPhP mode. From Figure 2, it is vivid to see the two regions where the imaginary surface conductivity is positive and negative, which respectively give the possibility of TM and TE SPhP modes within the polar crystal. It is intuitive to expect TM (TE) SPhP to be strongest where the magnitude of imaginary surface conductivity is large. Therefore, these regions play important roles in the analysis of surface polaritons of this paper.

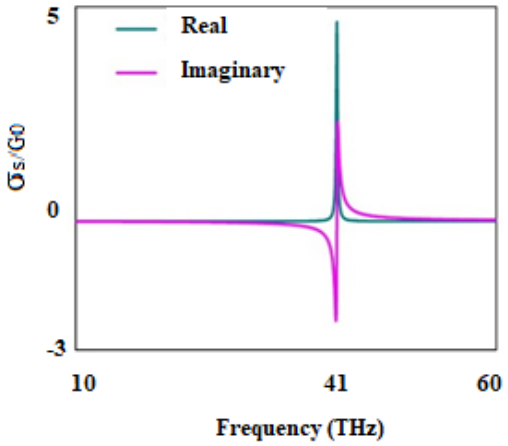

Figure 2: The dispersive surface conductivity of monolayer.

The Eq. (1) and Eq. (2) are called dispersion equations, which gives the relationship between propagation wave vector to the frequency. In Figure 3, the quantity $Re\,(k_x) \times {}^{c}/_{\omega}$ called effective mode index is plotted with frequency for both TM in Figure 3(a) and TE in Figure 3(b).

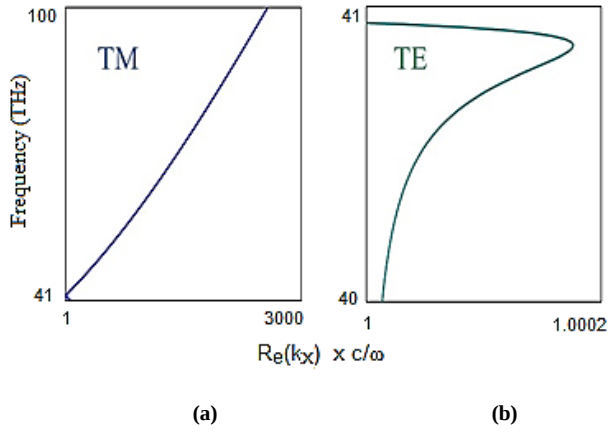

(a) **(b)**

Figure 3: The dispersion relations of the monolayer hBN: a) transverse magnetic b) transverse electric phonon polaritons.

From the Figure 3, the effective mode index of TM SPhP reaches approximate value of ~3000. Remarkably it is only ~1.0002 for TE SPhP. The values of effective mode index give light confinement of the surface wave with reference to the incident energy. Based on that, one can conclude that TM SPhP mode confined energy at the surface of monolayer hBN much tighter than TE SPhP mode. The analytical meaning of these is the ability to design efficient and sub-diffraction optoelectronics devices. For the TE polaritons, the weak value of effective mode index highlights weakly confined modes that can be difficult to utilize in a strong-field related optoelectronics devices. This led to the utilization of TM polaritons in optical communication and optoelectronics devices with strong confinement of electromagnetic energy such as solar cell, waveguides, and many more.

However, due to interesting finding by (Musa et al., 2017), the TE polaritons in hBN will find applications in nano waveguides and nanophotonics devices. The skin-depth engineering can be employed to define the vertical energy penetration into nanomaterial layer. It gives an idea the depth of the electromagnetic energy that is penetrated into the nanocrystal. For the device engineers it gives insight into how far the crystal can be integrated into the realistic device, such as nano wave guiding, sub-diffraction routing, and nanofibers. The simple expression of skin-depth can be written as $\delta_{hBN} = 1/Im(k_z)$ where k_z is the transverse wave vector. Figure 4 shows the analytical plot of dispersive skin-depth of TM in Figure 4(a) and for TE in Figure 4(b). The value can be as small as $0.27\lambda_0$ for TM SPhP and as big as $5\lambda_0$ for TE SPhP.

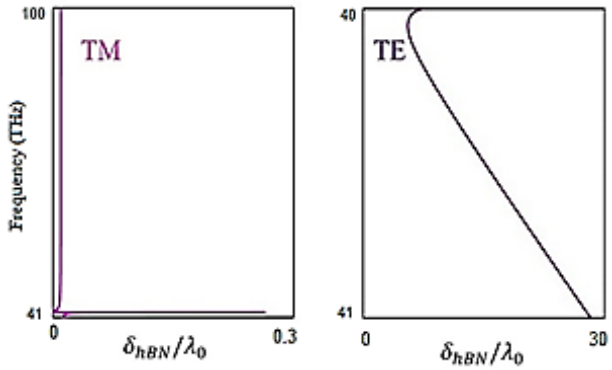

(a) **(b)**

Figure 4: The skin depth of suspended monolayer hBN: a) TM SPhP, b) TE SPhP.

In optoelectronic applications, the distance of which the electromagnetic energy travels without decaying is significant, and is called propagation length. In most of electronics and photonics analysis, it is the figure of merits that quantifies the distance of which the electromagnetic wave travelled. The inverse damping factor $\frac{Re(k_x)}{Imag(k_x)} = 4\pi \frac{L_p}{\lambda_{SPhP}}$ is the dimensionless quantity that relates propagation length (L_p) and effective polaritons wavelength (λ_{SPhP}). In the expression, k_x is the propagation wavevector. From Figure 5, the inverse damping factor is plotted for both TM SPhP in

Figure 5(a) and Figure 5(b) for TE SPhP as a function of frequency. It is significant to observed that, the value of

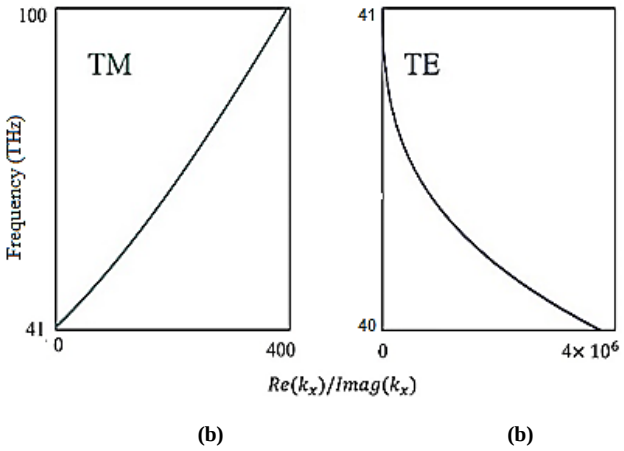

Figure 5: The propagation length of the phonon polaritons in monolayer hBN: a) TM SPhP, b) TE SPhP.

propagation loss keeps increasing with frequency for TM SPhP, while it is inverse for TE SPhP.

The physical interpretation of large value of inverse damping factor is the larger propagation length of the electromagnetic wave due to lower propagation loss. From this analysis, the TE SPhP exhibits larger inverse damping ratio as such possess longer propagation length. In practical optoelectronics or communication devices, this can be employed to design nanowaveguides, nanoresonators, or nanorouters that support both TE and TM modes.

IV. CONCLUSION

By numerically comparing these fundamental modes, we found that the TM phonon polaritons exhibit stronger confinement than the weaker confined TE phonon polaritons. The propagation length is intuitively longer in the TE phonon polaritons due to lower losses in TE polaritons. These important comparisons might facilitate greater understanding the properties of the two phonon polaritons modes, which improves their usage in the photonic and electronics devices. An extensive analysis is performed for the TM and TE SPhP in monolayer hBN crystal – a polar dielectric that exhibits Restsrahlen bands in Terahertz frequency. The structure is depicted to be suspended in air-filled half-spaces without considering effect of substrate and superstrate, to open the beginning of in-depth analysis. As expected TM SPhP exhibited tighter confinement and skin depth, while TE SPhP exhibited lower losses which make it strong candidate for waveguides and routing devices in communication and electronics devices. These findings proved that SPhP will fit well place in monolayer hBN as the good choice for optoelectronics, communication, and photonic devices.

REFERENCES

AbdEl-hameed, R. S. (2011). Aminolysis of Polyethylene Terephthalate Waste as Corrosion Inhibitor for Carbon Steel in HCl Corrosive medium. Advances in Applied Science Research, 2(3): 483 – 499.

Abeng, F. E.; V. D. Idim and P. J. Nna. (2017). Kinetics and thermodynamnic study of corrosion inhibitor of mild steel using methanolic extract, World news of natural sciences, 10: 26 – 38.

Andreani, S.; M. Znini; L. Paolini; J. Majidi; B. Hammouti, J. Costa1 and A. Muselli. (2016). Study of corrosion inhibition for mild steel in hydrochloric acid solution by limbarda crithmoides (l.) Essential oil of corsica, Journal of Mater. Environ. Sci. 7 (1): 187-195.

Basov, D. N.; M. M. Fogler; and F. J. García de Abajo. (2016). Polaritons in van der Waals materials. Science, 354(6309): aag1992.

Caldwell, J. D.; L. Lindsay; V. Giannini; I. Vurgaftman; T. L. Reinecke; S. A. Maier; and O. J. Glembocki. (2015). Low-loss, infrared and terahertz nanophotonics using surface phonon polaritons. Nanophotonics, 4(1): 44-68.

Cassabois, G.; P. Valvin and B. Gil. (2016). Hexagonal boron nitride is an indirect bandgap semiconductor. Nature Photonics, 10: 262–266.

Dai, S.; Z. Fei; Q. Ma; A. S. Rodin; M. Wagner; A. S. McLeod; M. K. Liu; W. Gannett; W. Regan; K. Watanabe; and T. Taniguchi. (2014). Tunable phonon polaritons in atomically thin van der Waals crystals of boron nitride. Science, 343(6175):1125-1129.

Ha, D. T.; T. T. Dinh; T. H. Vo; T. T. V. Tran; and A. V. Nguyen. (2017). On the theory of three types of polaritons (phonon, exciton and plasmon polaritons). In Journal of Physics: Conference Series, 865(1): 012007.

Hong, F. and Blaikie, R. (2019). Plasmonic Lithography: Recent Progress. Advanced Optical Materials, 7(14):1801653.

Kim, K.K., A. Hsu; X. Jia; S. M. Kim; Y. Shi; M. Hofmann; D. Nezich; J. F. Rodriguez-Nieva; M. Dresselhaus; T. Palacios and J. Kong. (2012). Synthesis of Monolayer Hexagonal Boron Nitride on Cu Foil Using Chemical Vapor Deposition. Nano Letters, 12:161−166.

Lee, S.C.; S. S. Ng; H. A. Hassan; Z. Hassan and T. Dumelow. (2014). Crystal orientation dependence of polarized infrared response of sapphire crystal. Optical Materials, 37: 773-9.

Lee, S.C.; S. S. Ng; H. A. Hassan; Z. Hassan and T. Dumelow. (2015). Surface phonon polaritons responses of hexagonal sapphire crystals with non-polar and semi-polar crystallographic planes. Optics Letters, 39(18): 5467-5470.

Lin, X.; Y. Shen; I. Kaminer; H. Chen and M. Soljacic. (2017). Transverse-electric Brewster effect enabled by nonmagnetic two-dimensional materials. Physical Review A, 94:023836.

Low, T., A. Chaves; J. D. Caldwell; A. Kumar; N.X. Fang; P. Avouris; T. F. Heinz; F. Guinea; L. Martin-Moreno and F. Koppens. (2017). Polaritons in layered two-dimensional materials. Nature materials, 16(2): 182-194.

Mak, K. F. and Shan, J. (2016). Photonics and optoelectronics of 2D semiconductor transition metal dichalcogenides. Nature Photonics, 10(4): 216-226.

Musa, M.Y.; M. Renuka; X. Lin; R. Li; H. Wang; E. Li; B. Zhang and H. Chen. (2017). Confined transverse electric

phonon polaritons in hexagonal boron nitrides. 2D Materials, 5(1):015018, 2017.

Poddubny, A.; I. Iorsh; P. Belov and Y. Kivshar. (2013). Hyperbolic metamaterials. Nature Photonics, 7:948–957.

Shi, G.; Y. Hanlumyuang; Z. Liu; Y. Gong; W. Gao; B. Li; J. Kono; J. Lou; R. Vajtai; P. Sharma and P. M. Ajayan. (2014). Boron Nitride−Graphene Nano capacitor and the Origins of Anomalous Size Dependent Increase of Capacitance. Nano Letters; 14(4): 1739–1744.

Wickramaratne, D.; L. Weston and C. G Van de Walle. (2018). Monolayer to bulk properties of hexagonal boron nitride. The Journal of Physical Chemistry C, 122(44): 25524-25529.

Woessner, A.; M. B. Lundeberg; Y. Gao; A. Principi; P. Alonso-González; M. Carrega; K. Watanabe; T. Taniguchi; G. Vignale; M. Polini and J. Hone. (2015). Highly confined low-loss plasmons in graphene–boron nitride heterostructures. Nature Materials, 14:421–425.

Zhang, J.; L. Zhang and W. Xu. (2012). Surface plasmon polaritons: physics and applications. Journal of Physics D: Applied Physics, 45(11): 113001.

Zhang, T. and Shan, F. (2014). Development and application of surface plasmon polaritons on optical amplification. Journal of Nanomaterials, 81(2): 221-229.